

AD-785 239

APPROXIMATE ANALYSIS OF HEAT TRANSFER
IN TRANSPIRED BOUNDARY LAYERS AT
LIMITING PRANDTL NUMBERS

Tse-Fou Zien

Naval Ordnance Laboratory
White Oak, Maryland

1 July 1974

DISTRIBUTED BY:

NTIS

National Technical Information Service
U. S. DEPARTMENT OF COMMERCE
5285 Port Royal Road, Springfield Va. 22151

UNCLASSIFIED

SECURITY CLASSIFICATION OF THIS PAGE (When Data Entered)

REPORT DOCUMENTATION PAGE		READ INSTRUCTIONS BEFORE COMPLETING FORM
1. REPORT NUMBER NOLTR 74-121	2. GOVT ACCESSION NO.	3. RECIPIENT'S CATALOG NUMBER AD-785 239
4. TITLE (and Subtitle) APPROXIMATE ANALYSIS OF HEAT TRANSFER IN TRANSPIRED BOUNDARY LAYERS AT LIMITING PRANDTL NUMBERS		5. TYPE OF REPORT & PERIOD COVERED
7. AUTHOR(s) TSE-FOU ZIEN		6. PERFORMING ORG. REPORT NUMBER
9. PERFORMING ORGANIZATION NAME AND ADDRESS Naval Ordnance Laboratory White Oak, Silver Spring, Maryland 20910		10. PROGRAM ELEMENT, PROJECT, TASK AREA & WORK UNIT NUMBERS 61152N; R00-001; ZR02302010; MAT-03L-000-199-31
11. CONTROLLING OFFICE NAME AND ADDRESS		12. REPORT DATE 1 July 1974
		13. NUMBER OF PAGES 33
14. MONITORING AGENCY NAME & ADDRESS (if different from Controlling Office)		15. SECURITY CLASS. (of this report) UNCLASSIFIED
		15a. DECLASSIFICATION/DOWNGRADING SCHEDULE
16. DISTRIBUTION STATEMENT (of this Report) Approved for public release; distribution unlimited.		
17. DISTRIBUTION STATEMENT (of the abstract entered in Block 20, if different from Report)		
18. SUPPLEMENTARY NOTES		
19. KEY WORDS (Continue on reverse side if necessary and identify by block number) Heat Transfer, Mass Transfer, Laminar Boundary Layers, Prandtl Number Effect, Approximate Method		
20. ABSTRACT (Continue on reverse side if necessary and identify by block number) A simple procedure is developed for approximate calculations of wall heat-transfer rates in transpired boundary layers. Applications of this procedure are illustrated by various examples of incompressible, laminar flows in the limits of large and small Prandtl numbers. A distinguished limit of large Prandtl number and small mass-transfer rate is easily identified, and some limiting solutions are presented for the porous-plate configuration. Calculations for the cases with small Prandtl numbers explicitly		

DD FORM 1473

(1 JAN 73)

EDITION OF 1 NOV 68 IS OBSOLETE
S/N 0102-010-6001

UNCLASSIFIED

SECURITY CLASSIFICATION OF THIS PAGE (When Data Entered)

Reproduced by
NATIONAL TECHNICAL
INFORMATION SERVICE
U. S. Department of Commerce
Springfield VA 22151

UNCLASSIFIED

SECURITY CLASSIFICATION OF THIS PAGE(When Data Entered)

demonstrate the usefulness of the method in studying transient heat-conduction problems. The remarkable combination of accuracy and simplicity represents the principal merit of the method.

//

UNCLASSIFIED

SECURITY CLASSIFICATION OF THIS PAGE(When Data Entered)

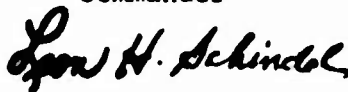
1 July 1974

APPROXIMATE ANALYSIS OF HEAT TRANSFER IN TRANSPIRED BOUNDARY
LAYERS AT LIMITING PRANDTL NUMBERS

This report presents a simple analytical procedure for approximate calculations of wall heat-transfer rates in transpired laminar boundary layers at limiting Prandtl numbers. The work represents a further extension of the investigation by Zien (NOLTR 73-17) on heat-transfer calculations at moderate Prandtl numbers. The simplicity and accuracy continue to be the principal merits of the method.

This study was conducted under the sponsorship of NOL Independent Research Project, Task Number MAT 03L-000/ZR02302/010.

ROBERT WILLIAMSON II
Captain, USN
Commander



LEON H. SCHINDEL
By direction

CONTENTS

	Page
INTRODUCTION.....	1
GENERAL FORMULATION.....	2
Equations and Boundary Conditions.....	2
Present Method of Solution.....	3
APPLICATION TO CASES OF LARGE Pr	4
General Remarks.....	4
Porous Plate: Similarity Case.....	5
A Distinguished Limit.....	7
Porous Plate: Similarity Case.....	9
Porous Plate: Nonsimilar Case.....	9
APPLICATION TO CASES OF SMALL Pr	10
General Remarks.....	10
Porous Plate: $\epsilon = \text{const.} = 0(1/\sqrt{R_x Pr})$	11
Circular Cylinder.....	12
Two-Dimensional Stagnation Point, Uniform V_w	13
CONCLUDING REMARKS.....	15
Acknowledgements.....	16
REFERENCES.....	16

ILLUSTRATIONS

Figure	Title
1	Porous Plate, Similarity Case, $Pr = 1$ (Present Method, $u = y \tau_w/\mu$)
2	Porous Plate, Similarity Blowing (Present Method, $u = y \tau_w/\mu$)
3	Porous Plate, Similarity Blowing (Present Method, $u = y \tau_w/\mu$)
4	Porous Plate, Similarity Suction (Present Method, $u = y \tau_w/\mu$)
5	Porous Plate, Similarity Blowing (Usual K-P Method, $u = y \tau_w/\mu$)
6	Porous Plate, Distinguished Limit for Similarity Case (Present Method)
7	Porous Plate, Distinguished Limit for Uniform ϵ (Present Method)
8	Porous Plate, Uniform ϵ , $Pr \rightarrow 0$ (Present Method)
9	Plane Stagnation Point, Uniform V_w , $Pr \rightarrow 0$ (Present Method)

SYMBOLS

a	radius of a circular cylinder
C_f	skin-friction coefficient, $\tau_w / \frac{1}{2} \rho u_\infty^2$
C_p	specific heat of gas at constant pressure
erfc	complementary error function
F	$\frac{1}{2} C_f$
g	profile for dimensionless temperature, $\frac{T - T_\infty}{T_w - T_\infty}$
$g_1(\eta)$	$1 - \eta$
$g_4(\eta)$	$1 - 2\eta + 2\eta^3 - \eta^4$
K-P	Karman-Pohlhausen
k	heat conductivity of the gas
N_x	Nusselt number $\dot{q}_w x / (T_w - T_\infty) k$
N_D	Nusselt number, $2a \dot{q}_w / (T_w - T_\infty) k$
Pr	Prandtl number, $\mu C_p / k$
\dot{q}	heat flux in the direction of y
R_D	Reynolds number based on the diameter, $2u_\infty a / \nu$
R_x	Reynolds number based on x , $u_\infty x / \nu$
R_δ	Reynolds number based on δ , $u_\infty \delta / \nu$
R_T	Reynolds number based on δ_T , $u_\infty \delta_T / \nu$
T	absolute temperature
(u, v)	velocity components corresponding to (x, y)
(u^*, v^*)	$(u/u_\infty, v/u_\infty)$
(x, y)	orthogonal coordinate system with origin at the leading edge or forward stagnation point, x along the surface
(α, β, γ)	velocity profile-parameters defined in Ref. (1)
$\tilde{\alpha}$	a temperature profile-parameter,

$$\int_0^1 \eta_T g(\eta_T) d\eta_T + \frac{1}{2} \int_0^1 \eta_T^2 g(\eta_T) d\eta_T - \int_0^1 d\eta_T \int_0^{\eta_T} \eta_T g(\eta_T) d\eta_T$$

$\tilde{\alpha}_1$

a temperature profile-parameter,

$$\int_0^1 g(\eta_T) d\eta_T - \int_0^1 d\eta_T \int_0^{\eta_T} g(\eta_T) d\eta_T + \int_0^1 \eta_T g(\eta_T) d\eta_T$$

 $\tilde{\beta}$

a temperature profile-parameter,

$$\int_0^1 g(\eta_T) d\eta_T$$

 $\tilde{\gamma}$

a temperature profile-parameter,

$$\int_0^1 \eta_T g(\eta_T) d\eta_T$$

 δ

thickness of velocity boundary layer

 δ_T

thickness of thermal boundary layer

 ϵ

 basic mass-transfer parameter, v_w/u_e
 η_T

 similarity variable, y/δ_T
 θ

 dimensionless temperature, $\frac{T - T_\infty}{T_w - T_\infty}$
 κ

 thermal diffusivity, $k/(\rho C_p)$
 Λ
 $\tilde{\lambda} Pr^{-2/3}$
 Λ_1
 $Pr \lambda_1$
 λ
 $\epsilon x/\delta$
 $\tilde{\lambda}$
 $\epsilon R_x^{1/2}$
 λ_1
 ϵR_T
 $\tilde{\lambda}_1$
 $\epsilon (R_x Pr)^{1/2}$
 μ

dynamic viscosity

 ν

kinematic viscosity

 ρ

density

 τ

shear stress

 ϕ

angle measured from forward stagnation point

Subscripts

∞	condition far upstream
e	edge of boundary layer
w	wall condition
0	initial condition

INTRODUCTION

A simple, approximate method for calculating the skin friction on porous surfaces has recently been described by Zien (Refs. (1) and (2)). It is based on an idea, due originally to Volkov (Ref. (3)), for refining the classical Karman-Pohlhausen (K-P) momentum integral technique in the boundary-layer theory, and is basically a one-parameter type of integral approach.

The chief merits of this analytical method, as illustrated in References (1) and (2), lie in the remarkable combination of simplicity and accuracy. The relative insensitivity of the results to the choice of velocity profiles is particularly noteworthy. These encouraging findings are indicative of the potential of the method for development into a useful tool for practical calculations of boundary-layer flows of a more complex nature. Further exploitation and extension of this new method appear warranted.

This paper presents a procedure for approximate calculations of wall heat-transfer in a transpired boundary layer at extreme Prandtl numbers. The procedure is based on a further modification and extension of Volkov's (Ref. (3)) original idea. Thus, the heat transfer on an aerodynamic surface is calculated by considering the energy balance across the entire, attendant (thermal) boundary layer at a local flow station. A second integration of the energy equation in the direction normal to the surface is then performed to provide an ordinary differential equation for the determination of the basic profile-parameter. To be sure, the idea of using a double-integration scheme had appeared earlier in Whitehead's (Ref. (4)) investigation of momentum boundary layers. However, the determination of skin friction in Reference (4) was based on the local slope of the assumed velocity profile, as in the original K-P procedure.

For easy demonstration of the method, only simple, yet basic, flows are considered in this paper. Thus, applications are made to two-dimensional, incompressible, laminar boundary layers of a single-component fluid. Results are presented here only for limiting cases of large or small Prandtl numbers where certain simplifying approximations can be effectively exploited to further facilitate the exhibition of the central ideas of the method. Detailed results for $Pr = 0(1)$ pertaining to the semi-infinite flat plate with uniform surface mass flux are available in Reference (5). The frictional heating is neglected in the energy equation throughout the calculations, and this approximation is generally valid for incompressible boundary layers where the Eckert number is usually small. An exact and comprehensive analysis of heat transfer in a class of self-similar transpired boundary layers, including the effects of frictional heating, can be found in Gersten and Korner (Ref. (6)).

The method is first applied to the case of transpired boundary layers with large Prandtl numbers. A distinguished limit of large Prandtl number and small mass-transfer rate is readily apparent in the present integral formulation. Some examples of this limiting flow are studied. The procedure is then used to study a class of low Prandtl number heat-transfer problems, and the usefulness of the present method in providing approximate solutions to general transient heat-conduction problems becomes evident in the process.

It is noted here that all the calculations presented in this paper involve, at most, the numerical integration of a single, first-order ordinary differential equation. In many cases solutions are obtained in explicit, analytical forms. The primary purpose of the paper is not to present solutions to any new problems. Rather, it is to show how simply some old solutions can be reproduced with good accuracy by the present method.

GENERAL FORMULATION

Equations and Boundary Conditions

In terms of the nondimensional velocity (u^*, v^*) and temperature, θ , the basic differential equations and boundary conditions for an incompressible, constant-property, laminar boundary layer over an isothermal porous surface are:

$$\frac{\partial u^*}{\partial x} + \frac{\partial v^*}{\partial y} = 0 \quad , \quad (1a)$$

$$u^* \frac{\partial u^*}{\partial x} + v^* \frac{\partial u^*}{\partial y} = \frac{v}{u_\infty} \frac{\partial^2 u^*}{\partial y^2} + u_e^* \frac{\partial u_e^*}{\partial x} \quad , \quad (1b)$$

$$u^* \frac{\partial \theta}{\partial x} + v^* \frac{\partial \theta}{\partial y} = \frac{v}{u_\infty} \frac{1}{Pr} \frac{\partial^2 \theta}{\partial y^2} \quad ; \quad (1c)$$

at $y = 0$:

$$u^* = 0 \quad (2a)$$

$$\theta = 1 \quad (2b)$$

$$v^* = \epsilon \quad (2c)$$

as $y \rightarrow \infty$:

$$u^* \rightarrow 1 \quad (2d)$$

$$\theta \rightarrow 0 \quad (2e)$$

In the usual practice of integral methods, the asymptotic conditions are specified at the edges of the boundary layer, δ and δ_T , for u^* and θ , respectively. Some initial conditions on u^* and θ are generally required at $x = 0$ to complete the formulation. These initial conditions are replaced by conditions on initial boundary-layer thicknesses, $\delta(0)$ and $\delta_T(0)$, in the present integral formulation.

The skin-friction coefficient, C_f , and the Nusselt number, N_x , are related to u^* and θ through the following expressions:

$$\frac{1}{2}C_f = \frac{\nu}{u_\infty} \left. \frac{\partial u^*}{\partial y} \right|_w \quad (3a)$$

and

$$N_x = -x \left. \frac{\partial \theta}{\partial y} \right|_w \quad (3b)$$

Present Method of Solution

Since the momentum equation is decoupled from the energy equation, the solution of u^* can proceed independently of the temperature field. In order to present a self-consistent development of the calculation procedure, we shall make use of the approximate solutions of u^* by a similar calculation scheme as reported by References (1) and (2) for the examples to be discussed below.

We now proceed directly to solve the energy equation. The first integration of (1c) gives

$$\frac{\partial}{\partial x} \int_0^y u^* \theta dy + \epsilon(\theta - 1) - \theta \frac{\partial}{\partial x} \int_0^y u^* dy = \frac{\kappa}{u_\infty} \left(\frac{\partial \theta}{\partial y} - \left. \frac{\partial \theta}{\partial y} \right|_w \right) \quad (4)$$

where the continuity equation has been used to eliminate v^* in favor of u^* .

Equation (4) is taken as an expression for the wall heat flux by letting the integration cover the entire thermal boundary layer. Thus, using (3b), we have

$$S_t \equiv \frac{N_x}{R_x Pr} = \frac{d}{dx} \int_0^{\delta_T} u^* \theta dy - \epsilon \quad (5)$$

Equation (5) is a nondimensional version of the energy balance across the thermal boundary layer at the station x .

Therefore, the surface heat transfer is determined from an integral expression involving the assumed profiles for u^* and θ . Of course, this representation would be exactly the same as the one using the derivative of θ at the wall if the profiles used for u^* and θ were the exact solutions of the problem under consideration.

The basic parameter of the thermal boundary layer, δ_T , is to be determined by the following differential equation which results from a second integration of the original energy equation. Thus, effecting another integration of (4), we arrive at

$$\int_0^{\delta_T} dy \frac{\partial}{\partial x} \int_0^y u^* \theta dy + \int_0^{\delta_T} \left(\epsilon - \frac{\partial}{\partial x} \int_0^y u^* dy \right) \theta dy = \delta_T \frac{d}{dx} \int_0^{\delta_T} u^* \theta dy - \frac{\kappa}{u_\omega} \quad (6)$$

In deriving (6) use has been made of the wall heat-flux expression, (5).

We assume the following simple form for θ :

$$\theta = g(\eta_T) = \sum_{i=0}^n k_i \eta_T^i, \quad k_i = \text{const} \quad (7)$$

The choice of the profiles is obviously crude in the sense that they presume similarity for general flows to be considered below. However, they are to be chosen such that the essential boundary conditions, (2b) and (2e), are observed.

Equation (6) reduces to a first-order, nonlinear, ordinary differential equation for δ_T , once a form for θ , such as (7), is introduced. With δ_T solved, the Stanton number, S_t , follows readily from (5) through an algebraic process.

APPLICATION TO CASES OF LARGE Pr

General Remarks

The existing literature on boundary-layer flows with large Prandtl numbers is voluminous. Our purpose here is merely to describe the application of the present simple method to this class of flows. Hence, only the references pertinent to the present development and results will be mentioned.

For large Prandtl numbers, the simplified representation of the velocity in the thermal boundary layer is

$$u \sim \frac{\tau_w}{\mu} y \quad (8)$$

This approximation was introduced and established by Fage and Falkner (Ref. (7)), Lighthill (Ref. (8)), Morgan and Warner (Ref. (9)), among others, and is convenient for systematic developments. Subsequent extensions and improvements of this simplifying approximation can be found, for example, in Curle (Ref. (10)), and more recently, Chao (Ref. (11)). This simple expression will be exploited in the present formulation. The examples to be presented here are porous-plate boundary layers for which the skin friction, τ_w , has been calculated earlier by Zien (Refs. (1) and (2)). A self-consistent development of the procedure is thus readily accessible. The results to be presented and discussed in the following are all based on the approximate solutions of τ_w pertaining to the linear velocity profile used in Reference (1). However, two temperature profiles, g_1 and g_4 , are used in the calculation to test the sensitivity of results to the temperature profiles. We note here that the velocity profile-parameters take the values $(\alpha, \beta, \gamma) = (1/8, 1/2, 1/6)$ in the ensuing calculations (see Ref. (1)), and the temperature profile-parameters, (α, β, γ) for g_1 and g_4 are $(1/8, 1/2, 1/6)$ and $(1/28, 3/10, 1/15)$, respectively.

Porous Plate: Similarity Case

The basic equations are (5) and (6). From (8) we have

$$u^* = \frac{1}{2} C_f R_T n_T = F R_T n_T \quad (9)$$

where $R_T = u_\infty \delta_T / \nu$. For this particular flow, the result of F as reported by Zien (Ref. (1)), i.e.,

$$F = R_X^{-1/2} \left(\frac{\alpha}{2} - \beta \lambda \right)^{-1/2} \left(\frac{\gamma}{2} - \lambda \right) \quad , \quad (10a)$$

will be used. Also, λ is related to $\tilde{\lambda}$ through

$$\tilde{\lambda} = \lambda \left(\frac{\alpha}{2} - \beta \lambda \right)^{-1/2} \quad . \quad (10b)$$

Substitution of (9) into (6) leads readily to

$$\tilde{\alpha} R_T \frac{d}{dR_X} (R_T^2 F) = \frac{1}{Pr} + \tilde{\beta} \epsilon R_T \quad . \quad (11)$$

For the case of similarity blowing (or suction), $\epsilon R_T = \text{const.}$, and (11) is easily integrated to give the following solution:

$$\lambda_1^3 - \left[\frac{2}{\tilde{\alpha}} \tilde{\beta} \tilde{\lambda}^3 \frac{(\frac{\alpha}{2} - \beta \lambda)^{1/2}}{(\frac{\gamma}{2} - \lambda)} \right] \lambda_1 - \frac{2}{\tilde{\alpha}} \frac{1}{Pr} \tilde{\lambda}^3 \frac{(\frac{\alpha}{2} - \beta \lambda)^{1/2}}{(\frac{\gamma}{2} - \lambda)} = 0, \quad (12)$$

where $\lambda_1 \equiv \epsilon R_T$.

The heat transfer is obtained from (5), once R_T is found. The result is

$$\frac{N_x}{\sqrt{R_x}} = \text{Pr} \left[\frac{\tilde{\gamma}}{2} \left(\frac{2}{\tilde{\alpha}} \right)^{2/3} \left(\frac{1}{\text{Pr}} + \lambda_1 \beta \right)^{2/3} \left(\frac{\alpha}{2} - \beta \lambda \right)^{-1/6} \left(\frac{\gamma}{2} - \lambda \right)^{1/3} \tilde{\lambda} \right]. \quad (13)$$

Equations (12), (13) and (10b) constitute the solution for $N_x/R_x^{1/2}$ as functions of λ and Pr .

It is interesting to note the behavior of the present approximate solutions in the limit of $\text{Pr} \rightarrow \infty$ and $\lambda = 0(1)$ for suction and blowing separately. Following limiting solutions are easily deduced from (12) and (13):

$$\tilde{\lambda} < 0 : \lambda_1 \sim -\frac{1}{\tilde{\beta}} \frac{1}{\text{Pr}} \quad \text{and} \quad \frac{N_x}{R_x^{1/2}} \sim |\tilde{\lambda}| \text{Pr} \quad ; \quad (14)$$

$$\tilde{\lambda} > 0 : \lambda_1 \sim \tilde{\lambda}^{3/2} \left[\frac{2\tilde{\beta}}{\tilde{\alpha}} \frac{(\frac{\alpha}{2} - \beta\tilde{\lambda})^{1/2}}{\frac{\gamma}{2} - \lambda} \right]^{1/2} \quad \text{and}$$

$$\frac{N_x}{R_x^{1/2}} \sim \text{Pr} \tilde{\lambda} \left(\frac{\tilde{\gamma}}{\tilde{\alpha}} \tilde{\beta} - 1 \right) \quad (15)$$

For the special case of $\tilde{\lambda} = 0$, the asymptotic limits for $N_x/R_x^{1/2}$ as $\text{Pr} \rightarrow \infty$ are $0.367 \text{Pr}^{1/3}$ and $0.338 \text{Pr}^{1/3}$ for $\theta = g_1$ and g_4 , respectively. These approximate limits are to be compared with the exact limit of $0.339 \text{Pr}^{1/3}$ (see, for example, Ref. (12)).

As $\text{Pr} \rightarrow \infty$, the heat-transfer rate predicted here approaches the correct asymptote (see Gersten and Körner, Ref. (6)) independent of profiles for the case of suction. For blowing, the present solutions show a strong profile-dependent behavior. Note that the quantity in the parenthesis of (15) is negative for both profiles considered here. The implications of the above observations are thus clear. As Pr increases, the present solutions are uniformly good for suction, but predict too rapid a decay in the heat-transfer rate for blowing, especially when λ is large.

Some typical results are illustrated in Figures 1-4 and compared with the available exact solutions due to Stewart and Prober (Ref. (13)), and Thompson (Ref. (14)) whenever appropriate.

Figure 1 shows the results for $Pr = 1$ for which an exact integral, $\theta = 1 - u^*$, holds. Exact solutions for heat transfer are thus available from the exact skin-friction results of Emmons and Leigh (Ref. (15)), or directly from Reference (13), for comparison. It is remarkable that the present procedure, suitable for large Prandtl numbers, yields very accurate results of heat transfer for $Pr = 1$. Of course, the finding that the validity of a calculation procedure designed for large Prandtl numbers actually extends into regions of moderate Prandtl numbers is not totally unexpected, (see Ref. (8)). We also note the insensitivity of the present results to the profiles used in the calculations.

Figures 2-4 show the heat-transfer results are functions of the Prandtl number at three values of $\tilde{\lambda}$: $\frac{0.01}{\sqrt{2}}$, $\frac{0.1}{\sqrt{2}}$ and $-\frac{\sqrt{2}}{10}$, for which exact solutions are available for comparison. These results clearly confirm our aforementioned predictions based on the behavior of the present solutions in the limit of $Pr \rightarrow \infty$. However, it should be remarked here that as $Pr \rightarrow \infty$, the results pertaining to blowing, though quantitatively inaccurate, are still qualitatively correct. It is possible that the thermal boundary layer is blown off the surface while the momentum boundary layer still remains attached.

The same approach and profiles are then employed in the original K-P procedure for this problem, using τ_w obtained from the original K-P method with a linear velocity profile, as reported in Reference (1). The results are presented here only for $\tilde{\lambda} = \frac{0.1}{\sqrt{2}}$ in Figure 5. A comparison between Figure 5 and Figure 3 clearly illustrates the superiority of the refined K-P procedure. The absence of a sharp decrease of the heat-transfer rate in the interval, $6 < Pr < 100$, is typical of the failure of the original K-P procedure. Nevertheless, it should be mentioned that for the case of suction, the original K-P procedure with the same profiles is also capable of predicting the correct asymptotic behavior for $Pr \rightarrow \infty$, only the sensitivity of results to profiles is more pronounced.

A Distinguished Limit

The singular perturbation nature of the boundary-layer energy equation in the limit of $Pr \rightarrow \infty$ is well-known. (See, for example, Narasimha and Vasantha, Reference (16). It is also apparent in (1c) in which the coefficient of the highest derivative approaches zero as $Pr \rightarrow \infty$. The asymptotic structure of the thermal boundary layer with surface blowing in the limit of $Pr \rightarrow \infty$ has been discussed

by Kassoy (Ref. (17)), among others. The interesting phenomenon of thermal layer blowoff is qualitatively analyzed for the case of a porous plate with similarity blowing in Reference (17).

Physically speaking, the thermal boundary layer has a vanishing thickness relative to the momentum boundary layer as $Pr \rightarrow \infty$, because the viscous diffusion ($\sim \nu$) dominates the thermal diffusion ($\sim \kappa$). Therefore, the heat transfer takes place in a very thin region close to the wall where the convective velocity components (u, v) are also small. In the case of transpired boundary layers, an additional mechanism of heat transfer ($\sim \epsilon$) appears. The precise orders of magnitude of these physical quantities as $Pr \rightarrow \infty$ are related uniquely only in a distinguished limit in which convection, conduction and mass transfer are of equal importance. It is convenient and instructive to deduce such a limit from the equations derived in the process of the present development. We remark here that, as $Pr \rightarrow \infty$, the present method seems particularly suited for this case of vanishingly small λ in view of the results discussed in the section of Porous Plate: Similarity Case.

Let us consider (11). The three terms from left to right represent, respectively, the effects of convection, conduction and mass transfer. Therefore, we require that, as $Pr \rightarrow \infty$,

$$\frac{R_T^3}{R_x^{3/2}} \sim \frac{1}{Pr} \sim \epsilon R_T, \quad (16)$$

where we have used the relation $F = O(R_x^{-1/2})$.

It follows immediately that

$$Pr \rightarrow \infty: \tilde{\lambda} = O(Pr^{-2/3}), \quad \lambda_1 = O(Pr^{-1}) \text{ and } \delta_T/\delta = O(Pr^{-1/3}). \quad (17)$$

Thus, the distinguished limit corresponds to vanishingly small values of $\tilde{\lambda}$ and δ_T/δ . We are now led to introduce the following variables for the study of this limiting flow:

$$\Lambda = Pr^{2/3} \tilde{\lambda} = O(1) \quad (18a)$$

$$\Lambda_1 = Pr \lambda_1 = O(1) \quad (18b)$$

In this limit, F may be expanded as

$$F = F_0 + \tilde{\lambda} F_1 + \dots \quad (19)$$

where F_0 corresponds to the skin-friction coefficient in the absence of mass transfer. Only the leading term, F_0 , will be needed in the ensuing calculations. The result to be obtained thus corresponds to an approximation of the leading asymptotic term in this distinguished limit. A systematic asymptotic analysis of the general flow in this distinguished limit appears to be an interesting problem of fundamental importance but beyond the scope of the present paper.

For a flat plate, Reference (1) provides

$$F_0 = \frac{\gamma}{\sqrt{2\alpha}} R_x^{-1/2} \quad (20)$$

and, as mentioned earlier, $(\alpha, \gamma) = (1/8, 1/6)$ is used in the calculations.

Porous Plate: Similarity Case

Introducing Λ and Λ_1 , and applying the limit process, (17), to (12) and (13), we arrive at the following results:

$$\Lambda_1^3 = (2)^{3/2} (\alpha)^{1/2} \Lambda^3 (1 + \Lambda_1 \tilde{\beta}) / (\tilde{\alpha} \gamma) \quad (21)$$

and

$$\frac{N_x}{R_x^{1/2}} = Pr^{1/3} \left[\tilde{\gamma} (\alpha)^{-1/6} (\tilde{\alpha})^{-2/3} (\gamma)^{1/3} (2)^{-1/2} (1 + \Lambda_1 \tilde{\beta})^{2/3} - \Lambda \right] \quad (22)$$

Results of $N_x / (R_x^{1/2} Pr^{1/3})$ as a function of Λ for the two temperature profiles are plotted in Figure 6. It can be shown that both curves approach the exact limit of asymptotic suction. The dependence of the results on profiles is still weak in this limiting flow, and the thermal boundary-layer blowoff ($N_x = 0$) is predicted at a finite value of Λ . An exact treatment of this limiting case was recently reported by Gersten (Ref. (18)) for a class of Falkner-Skan flows. The same distinguished limit was derived in a different manner in Reference (18). The exact solution pertaining to the flat-plate configuration is included in Figure 6 for comparison with the present approximate results. The agreement, in general, is clearly quite satisfactory, except near thermal boundary-layer blowoff where the exact solution exhibits an exponential decay in heat transfer.

Porous Plate: Nonsimilar Case

Equation (11) is still the basic differential equation for this nonsimilar flow, as the velocity, u , is approximated by (8). Now, applying the limit process, (17) and (18), to (11) and noting (20), we have the following differential equation for the limiting flow:

$$\frac{d\Lambda_1}{d\Lambda} = \frac{\frac{(8\alpha)^{1/2}}{\gamma\tilde{\alpha}} (1 + \tilde{\beta}\Lambda_1) + \left(\frac{\Lambda_1}{\Lambda}\right)^3}{2\left(\frac{\Lambda_1}{\Lambda}\right)^2} \quad (23a)$$

and

$$\Lambda \rightarrow 0, \quad \frac{\Lambda_1}{\Lambda} \rightarrow \frac{(8\alpha)^{1/6}}{(\gamma\tilde{\alpha})^{1/3}} \quad (23b)$$

Substituting (9) into (5) and introducing Λ and Λ_1 , we obtain

$$\frac{N_x}{R_x^{1/2}} = Pr^{1/3} \left[\frac{\tilde{Y}}{\tilde{\alpha}} \frac{\Lambda}{\Lambda_1} - \left(1 - \frac{\tilde{\beta}\tilde{Y}}{\tilde{\alpha}}\right)\Lambda \right] \quad (24)$$

Results of $N_x/(R_x^{1/2}Pr^{1/3})$ as a function of Λ are plotted in Figure 7 for the two temperature profiles used in the calculation. The behavior of heat transfer is quite analogous to that for the similarity case, Figure 6. We also note that the two curves will converge in the region of large negative Λ and approach the exact asymptotic suction limit,

$N_x/(R_x^{1/2}Pr^{1/3}) \sim |\Lambda|$. No other limiting solutions to this non-similar flow seem to exist in the literature, to the best of the author's knowledge.

APPLICATION TO CASES OF SMALL Pr

General Remarks

In this section, the method is applied to the calculation of boundary-layer heat transfer in the limit of $Pr \rightarrow 0$. The mathematical limit here is $R_x \rightarrow \infty$, $Pr \rightarrow 0$ and $R_x Pr \rightarrow \infty$, so that the concept of a thin thermal layer near the surface is still valid. The chief simplification is that the velocity profile, u , inside the thermal boundary layer can be approximated by the external potential stream $u_e(x)$, (Ref. (12)). Therefore, we need only to assume the temperature profile. The resulting solution corresponds to the limiting case of $Pr = 0$, i.e., an inviscid but heat-conducting fluid. Three representative examples will be presented in the following. These examples will explicitly reveal the relevance of the differential equations to a class of heat-conduction problems. Therefore, the success of the present method here would imply its potential usefulness in studying general

problems in transient heat conduction with complex boundary conditions, including nonlinear cases. Some initial attempts have already been made by Volkov and Li-Orlov (Ref. (19)). A more thorough investigation of this application appears desirable, and should lead to a modified version of the work of Goodman (Ref. (20)) who had applied the original K-P method to a variety of heat-conduction problems.

Porous Plate: $\epsilon = \text{const.} = 0(1/\sqrt{R_x \text{Pr}})$

Here the velocity $(u, v) = (u_\infty, v_w)$ and the energy equation takes the form

$$\frac{\partial \theta}{\partial x} + \epsilon \frac{\partial \theta}{\partial y} = \frac{\kappa}{u_\infty} \frac{\partial^2 \theta}{\partial y^2} \quad (25)$$

The first and second integrations of (25) lead to, respectively,

$$\frac{N_x}{R_x \text{Pr}} = \tilde{\alpha}_1 \frac{dR_T}{dR_x} - \epsilon \quad (26)$$

and

$$\tilde{\alpha}_1 \frac{dR_T}{dR_x} = \frac{1}{\text{Pr} R_T} + \epsilon \tilde{\beta} \quad (27)$$

where $(\tilde{\alpha}_1, \tilde{\beta})$ are profile-parameters defined in the Nomenclature. In deriving (26) and (27), a temperature profile of the form $\theta = g(\eta_T)$ is assumed. Equation (27) is readily integrated to give

$$\epsilon^2 R_x \text{Pr} = \frac{\tilde{\alpha}_1}{\tilde{\beta}} \epsilon R_T \text{Pr} - \frac{\tilde{\alpha}_1}{\tilde{\beta}^2} \ln(1 + \tilde{\beta} \epsilon R_T \text{Pr}) \quad (28)$$

and the heat-transfer coefficient follows from (26) as

$$\frac{N_x}{\sqrt{R_x \text{Pr}}} = \frac{\tilde{\beta}}{\tilde{\alpha}_1} \frac{\epsilon \sqrt{R_x \text{Pr}}}{\epsilon R_T \text{Pr}} - \left(1 - \frac{\tilde{\beta}^2}{\tilde{\alpha}_1}\right) \epsilon \sqrt{\text{Pr} R_x} \quad (29)$$

Equations (28) and (29) form a parametric representation for the heat-transfer coefficient, i.e.,

$$\frac{N_x}{\sqrt{R_x \text{Pr}}} = f(\epsilon \sqrt{R_x \text{Pr}}) \quad (30)$$

Results corresponding to the two temperature profiles, g_1 and g_4 , are illustrated in Figure 8. The profile-parameters associated with g_1 and g_4 and $(\tilde{\alpha}_1, \tilde{\beta}) = (1/3, 1/2)$ and $(2/15, 3/10)$, respectively.

It is interesting to note that (25) is also relevant to the problem of the transient heat conduction in a semi-infinite solid moving with a constant velocity ϵ and maintained at a constant temperature at $y = 0$. The exact solution is available in Carslaw and Jaeger (Ref. (21)). The heat-transfer rate is readily obtained from the solution for θ , i.e.,

$$\frac{N_x}{\sqrt{R_x Pr}} = \frac{1}{\sqrt{\pi}} \exp\left(-\frac{\epsilon^2 R_x Pr}{4}\right) - \frac{\epsilon \sqrt{R_x Pr}}{2} \operatorname{erfc}\left(\frac{\epsilon \sqrt{R_x Pr}}{2}\right) \quad (31)$$

The exact solution is also shown in Figure 8 for comparison with the approximate solutions, (30). The present results are clearly very satisfactory in accuracy; the close agreement between the results corresponding to the two temperature profiles is also evident. However, it should be pointed out that as the blowing intensity increases, the present approximate solutions predict zero heat transfer (thermal boundary-layer blowoff) at finite values of $\epsilon \sqrt{R_x Pr}$, while the exact solution shows exponential decay in heat transfer. Therefore, as is usually the case, the accuracy of the present solution begins to deteriorate as the blow-off point is approached.

Circular Cylinder

We now consider the case of a circular cylinder in crossflow. The orthogonal curvilinear coordinate system, (x, y) , has its origin at the forward stagnation point with x measuring the distance along the surface ($x = a\phi$). Then $u^* = 2\sin\phi$, $v^* = -2y^* \cos\phi$. The energy equation and the boundary conditions are

$$\sin\phi \frac{\partial \theta}{\partial \phi} - y^* \cos\phi \frac{\partial \theta}{\partial y^*} = \frac{1}{R_D Pr} \frac{\partial^2 \theta}{\partial y^{*2}} \quad (32a)$$

$$\theta(\phi, 0) = 1 \quad \theta(\phi, \delta_T^*) = 0 \quad , \quad (32b)$$

where $u^* = u/u_\infty$, $v^* = v/u_\infty$, $y^* = y/a$ and $\delta_T^* = \delta_T/a$.

Applying the present method to (32a) results in the following two equations, based on the assumed profile, $\theta = g(\eta_T)$:

$$\frac{1}{2} \frac{N_D}{R_D Pr} = \tilde{\beta} \left(\sin \phi \frac{d\delta_T^*}{d\phi} + \delta_T^* \cos \phi \right) \quad (33)$$

and

$$\delta_T^* \sin \phi \frac{d\delta_T^*}{d\phi} + \delta_T^{*2} \cos \phi = \frac{1}{\tilde{\alpha}_1} \frac{1}{R_D Pr} \quad (34a)$$

with

$$\delta_T^* (\phi, 0) = (\tilde{\alpha}_1 R_D Pr)^{-1/2} \equiv (\delta_T^*)_0 \quad (34b)$$

Equation (34a) can be easily integrated to give

$$\delta_T^* = (\delta_T^*)_0 \sec \frac{\phi}{2} \quad (35)$$

Equation (33) then gives

$$\frac{N_D}{\sqrt{R_D Pr}} = 2 \frac{\tilde{\beta}}{\sqrt{\tilde{\alpha}_1}} \cos \frac{\phi}{2} \quad (36)$$

$$= 1.73 \cos \frac{\phi}{2} \quad \text{for } \theta = g_1 \quad (37a)$$

$$= 1.64 \cos \frac{\phi}{2} \quad \text{for } \theta = g_4 \quad (37b)$$

The exact solution to this problem can be found in Grosh and Cess (Ref. (22)) who transformed the equation to a standard form of one-dimensional heat equation. The heat-transfer result is:

$$\frac{N_D}{\sqrt{R_D Pr}} = 1.60 \cos \frac{\phi}{2} \quad (38)$$

The present method is again shown to yield satisfactory results.

Two-Dimensional Stagnation Point, Uniform V_w

As a last example of this limiting flow, we consider the heat transfer near a plane stagnation point in the presence of uniform surface mass flux. Of course, the treatment is still within the framework of thermal boundary-layer theory.

Here we have $u = u_e = v_1 x$ and $v = v_w - y u_1$. The energy equation and the boundary conditions are

$$x^* \frac{\partial \theta}{\partial x^*} + (\tilde{\lambda}_1 - y^*) \frac{\partial \theta}{\partial y^*} = \frac{\partial^2 \theta}{\partial y^{*2}} \quad (39a)$$

$$\theta(x^*, 0) = 1, \quad \theta(x^*, \infty) = 0, \quad (39b)$$

where the coordinates and velocity are normalized by the characteristic length $\sqrt{\kappa/u}$, and velocity $\sqrt{\kappa u}$, respectively. In particular, we have

$$\tilde{\lambda}_1 \equiv \frac{v_w}{\sqrt{\kappa u_1}} = \frac{v_w}{u_e} \sqrt{\frac{u_e x}{\kappa}} = \epsilon \sqrt{R_x Pr} = O(1) \quad (40)$$

Using $\theta = g(\eta_T)$ and applying the present method to equation (39a) result in

$$\tilde{\alpha}_1 x^* \delta_T^* \frac{d\delta_T^*}{dx^*} + \tilde{\alpha}_1 \delta_T^{*2} = 1 + \tilde{\lambda}_1 \tilde{\beta} \delta_T^* \quad (41)$$

and

$$\frac{Nx}{\sqrt{R_x Pr}} \equiv \frac{q_w}{k} \frac{x}{T_w - T_\infty} \sqrt{\frac{\kappa}{u_e x}} = \tilde{\beta} (\delta_T^* + x^* \frac{d\delta_T^*}{dx^*}) - \tilde{\lambda}_1 \quad (42)$$

The solution to equation (41) is easily obtained as

$$\delta_T^* = \frac{1}{2\tilde{\alpha}_1} \left[\tilde{\beta} \tilde{\lambda}_1 + \sqrt{(\tilde{\lambda}_1 \tilde{\beta})^2 + 4\tilde{\alpha}_1} \right] = \text{const.} \quad (43)$$

Equation (42) then gives

$$\frac{Nx}{\sqrt{R_x Pr}} = \tilde{\beta} \delta_T^* - \tilde{\lambda}_1 \quad (44)$$

The exact solution to equation (39) is also easily obtained by noting that the boundary conditions and the original partial differential equation, (39a), admit a simple solution of the form $\theta = \theta(y^*)$. Hence, (39a) is essentially an ordinary differential equation whose solution has a simple closed-form. The exact heat transfer follows from the solution for θ , and is given by

$$\frac{Nx}{\sqrt{R_x Pr}} = \left[\int_0^{\infty} \exp \left(\tilde{\lambda}_1 y^* - \frac{1}{2} y^{*2} \right) dy^* \right]^{-1}$$

$$= \left[\sqrt{\frac{\pi}{2}} e^{\frac{\tilde{\lambda}_1^2}{2}} \left(1 + \operatorname{erf} \frac{\tilde{\lambda}_1}{\sqrt{2}} \right) \right]^{-1} \quad (45)$$

The approximate solutions have been obtained for two temperature profiles, g_1 and g_4 , and compared with the exact solution, equation (45), in Figure 9. Again, the approximate solutions are shown to be very accurate. It can further be shown analytically that the approximate solutions reduce to the exact asymptotic limit as $\tilde{\lambda}_1 \rightarrow -\infty$, independent of profiles. Near thermal boundary-layer blowoff, the comparison resembles closely that of the case of a porous plate studied in the Porous Plate section of this report.

CONCLUDING REMARKS

The primary purpose of this paper is to present a simple procedure for practical calculations of heat transfer in boundary layers. Oversimplified and, in fact, improper profiles are deliberately used in the calculations, and the principal merit of the method, namely, the remarkable combination of simplicity and accuracy, is amply demonstrated and fully exploited. No effort is expended here in providing the details of the flow field.

Results of these calculations indicate that the rudimentary application of the method, as described in this paper, is adequate for most engineering purposes. The weak dependence of the results to the profiles continues to prevail. This is believed to be a consequence of using an integral expression for the surface heat flux; the effect of improper profiles is mostly reflected in the somewhat spurious predictions of transverse scales of the boundary layers, δ and δ_T , so that the predictions of the wall heat-flux remain reasonably accurate. However, near the thermal boundary-layer blowoff where the heat-transfer rates are small, the results are useful only for qualitative purposes. This finding is reminiscent of the difficulty encountered in the previous skin-friction calculations (Refs. (1) and (2)).

The possibility of using the method to study general problems of transient heat conduction appears promising and warrants further investigation. In particular, the present method seems capable of providing simple approximate solutions to heat conduction problems with phase changes and moving boundaries, such as melting, ablations, etc. These problems have the characteristic feature of

nonlinear boundary conditions imposed on a (unknown) moving boundary. The technological importance of such problems is self-evident. The present approximate method should serve as a useful guide to the development of extensive numerical efforts in this area. Results of this study will appear in a separate report.

Acknowledgements

This research was supported by the Independent Research Program of the Naval Ordnance Laboratory. The author gratefully acknowledges some stimulating discussions with Professor K. Gersten of Ruhr University, Bochum, Federal Republic of Germany.

REFERENCES

1. Zien, T. F., "A New Integral Calculation of Skin Friction on a Porous Plate," AIAA Journal, 9, pp 1423-1425, 1971
2. Zien, T.F., "Skin Friction on Porous Surfaces Calculated by a Simple Integral Method," AIAA Journal, 10, pp 1267-1268, 1972
3. Volkov, V. N., "A Refinement of the Karman Pohlhausen Integral Method in Boundary-Layer Theory," Inzhenerno-Fizicheskii Zhurnal, 9, pp 583-588, 1965. (English translation in Journal of Engineering Physics, 9, pp 371-374)
4. Whitehead, L. G., "An Integral Relationship for Boundary Layer Flow," Aircraft Engineering, 21, pp 14-16, 1949
5. Zien, T. F., "An Approximate Calculation of Heat Transfer in Transpired Boundary Layers," NOLTR 73-17, Naval Ordnance Laboratory, Feb 1973
6. Gersten, K., and Körner, H., "Wärmeübergang unter Berücksichtigung der Reibungswärme bei laminaren Keilströmungen mit veränderlicher Temperatur und Normalgeschwindigkeit entlang der Wand," Int. J. Heat Mass Transfer, 11, pp 655-673, 1968
7. Fage, A. and Falkner, V. M., "Relation Between Heat Transfer and Surface Friction for Laminar Flow," ARC RM 1408, 1931
8. Lighthill, M. J., "Contributions to the Theory of Heat Transfer Through a Laminar Boundary Layer," Proceedings of the Royal Society, London, 202A, pp 359-377, 1950
9. Morgan, G. W. and Warner, W. H., "Heat Transfer in Laminar Boundary Layers at High Prandtl Number," Journal of the Aeronautical Sciences, 23, pp 937-948, 1956

10. Curle, N., The Laminar Boundary Layer Equations, Chap. 6, Clarendon Press, Oxford, 1962
11. Chao, B. T., "An Improved Lighthill's Analysis of Heat Transfer through Boundary Layers," Int. J. Heat Mass Transfer, 15, pp 907-920, 1972
12. Schlichting, H., Boundary Layer Theory, 6th Edition, Chap. 12, McGraw-Hill Co., New York, 1968
13. Stewart, W. E. and Prober, R., "Heat Transfer and Diffusion in Wedge Flows with Rapid Mass Transfer," Int. J. Heat Mass Transfer, 5, pp 1149-1163, 1962
14. Thompson, E. R., "High Prandtl Number Boundary Layers with Mass Injection," AIAA Journal, 7, pp 547-548, 1969
15. Emmons, H. W. and Leigh, D.C., "Tabulation of the Blasius Function with Blowing and Suction," ARC TR 15966, C.P. No. 157 1954
16. Narasimha, R. and Vasantha, S. S., "Laminar Boundary Layer on a Flat Plate at High Prandtl Number," ZAMP, 17, pp 585-592, 1966
17. Kassoy, D. R., "Injection Effects in High Prandtl Number Boundary-Layer Flows," AIAA Journal, 6, pp 1796-1797, 1968
18. Gersten, K., "Wärme- und Stoffübertragung bei großen Prandtl- bzw. Schmidtzahlen," Bericht Nr. 26/1973, Ruhr-Universität, Bochum, Germany (June 1973)
19. Volkov, V. N. and Li-Orlov, V. K., "A Refinement of the Integral Method in Solving the Heat Conduction Equation," Heat Transfer-Soviet Research, 2, pp 41-47, 1970
20. Goodman, T. R., "Application of Integral Methods to Transient Nonlinear Heat Transfer," Adv. Heat Transfer, 1, pp 55-122 1964
21. Carslaw, H. S. and Jaeger, J. C., Conduction of Heat in Solids, 2nd edition, Oxford University Press, Chap. 15, 388, 1959
22. Grosh, R. J. and Cess, R. D., "Heat Transfer to Fluids with Low Prandtl Numbers for Flow Across Plates and Cylinders of Various Cross Section," ASME Transaction, 80, pp 667-676, 1958

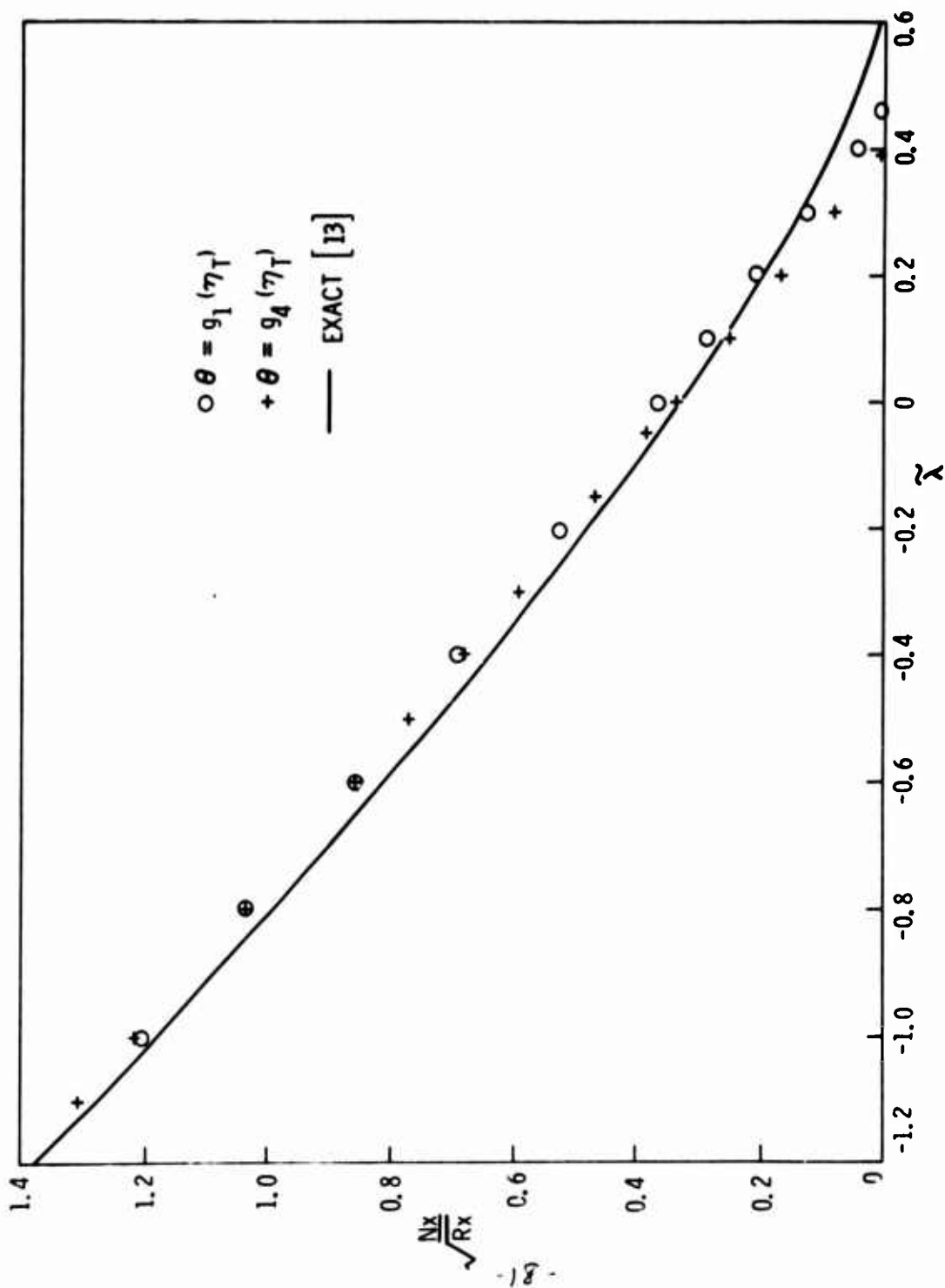


FIG. 1 POROUS PLATE, SIMILARITY CASE, $Pr = 1$ (PRESENT METHOD, $u = y\tau_w/\mu$)

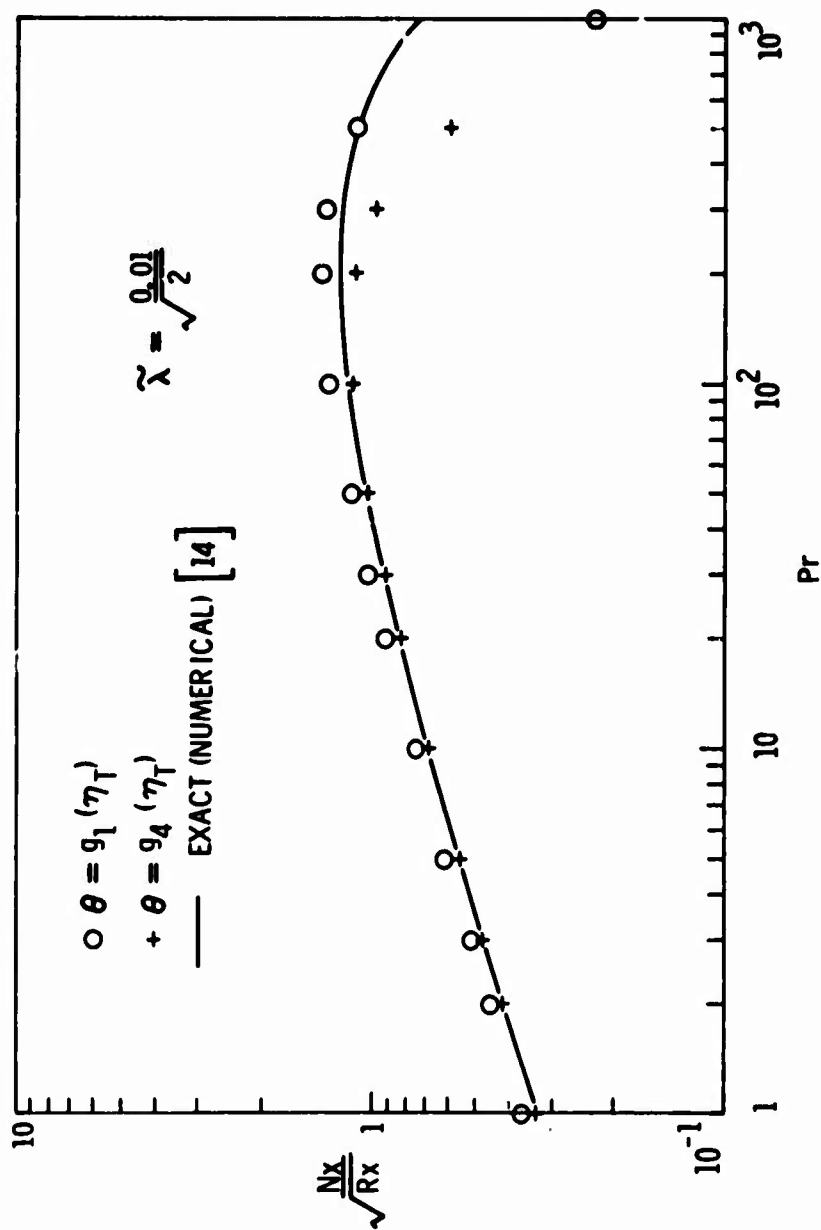


FIG. 2 POROUS PLATE, SIMILARITY BLOWING (PRESENT METHOD, $u = y\tau_w/\mu$)

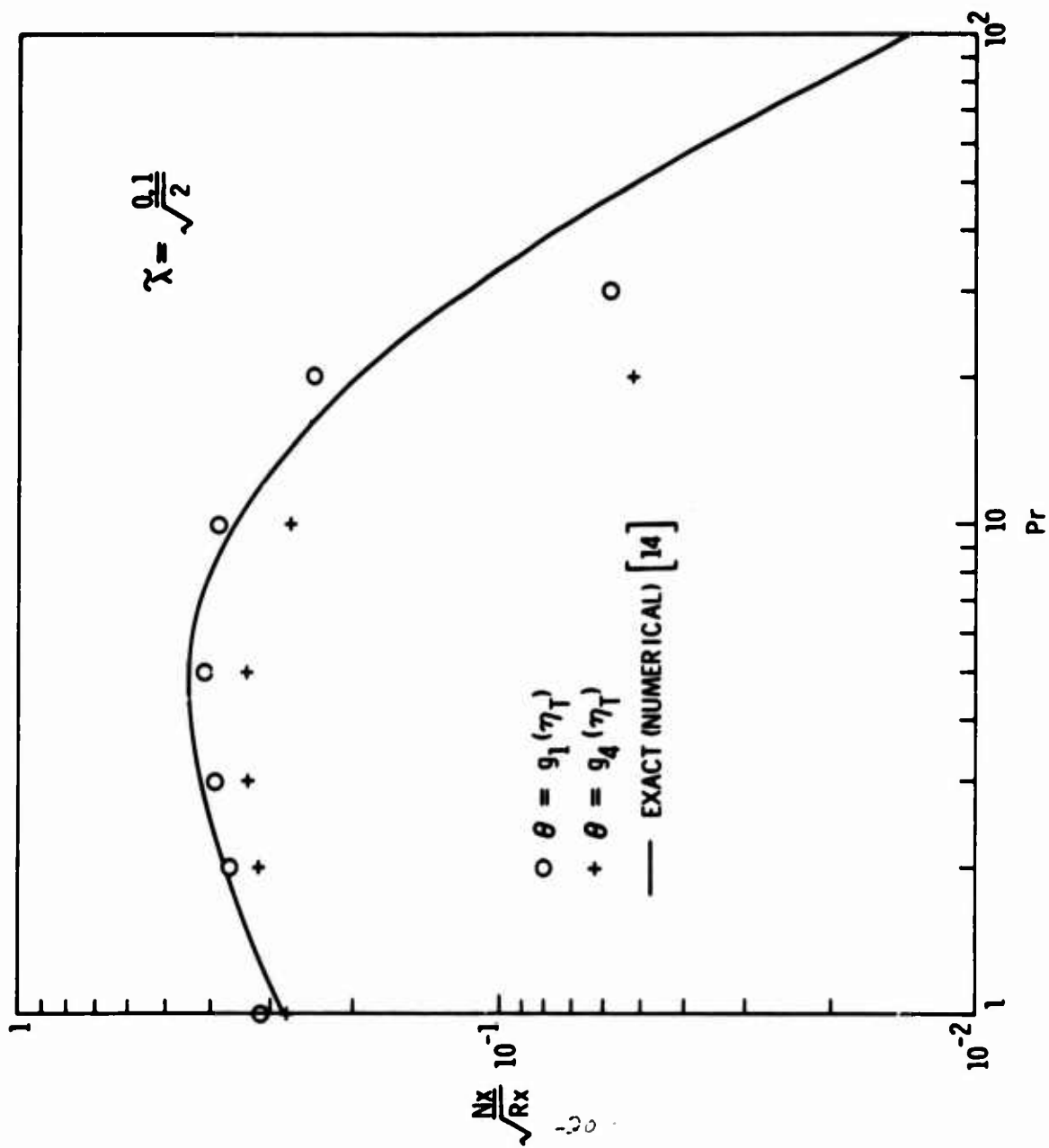


FIG. 3 POROUS PLATE, SIMILARITY BLOWING (PRESENT METHOD, $u = y \tau_w / \mu$)

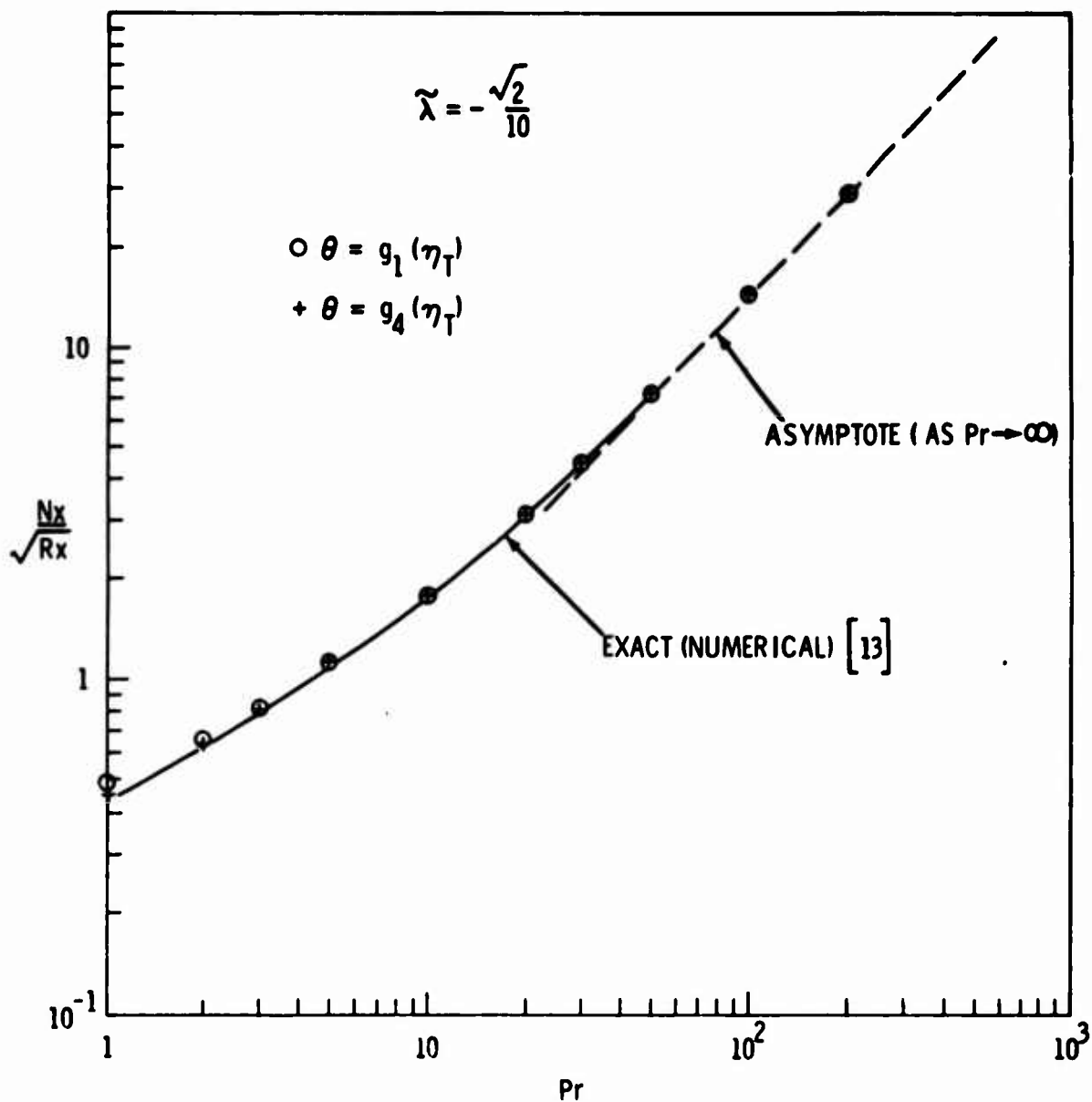


FIG. 4 POROUS PLATE, SIMILARITY SUCTION (PRESENT METHOD, $u = \gamma \tau_w / \mu$)

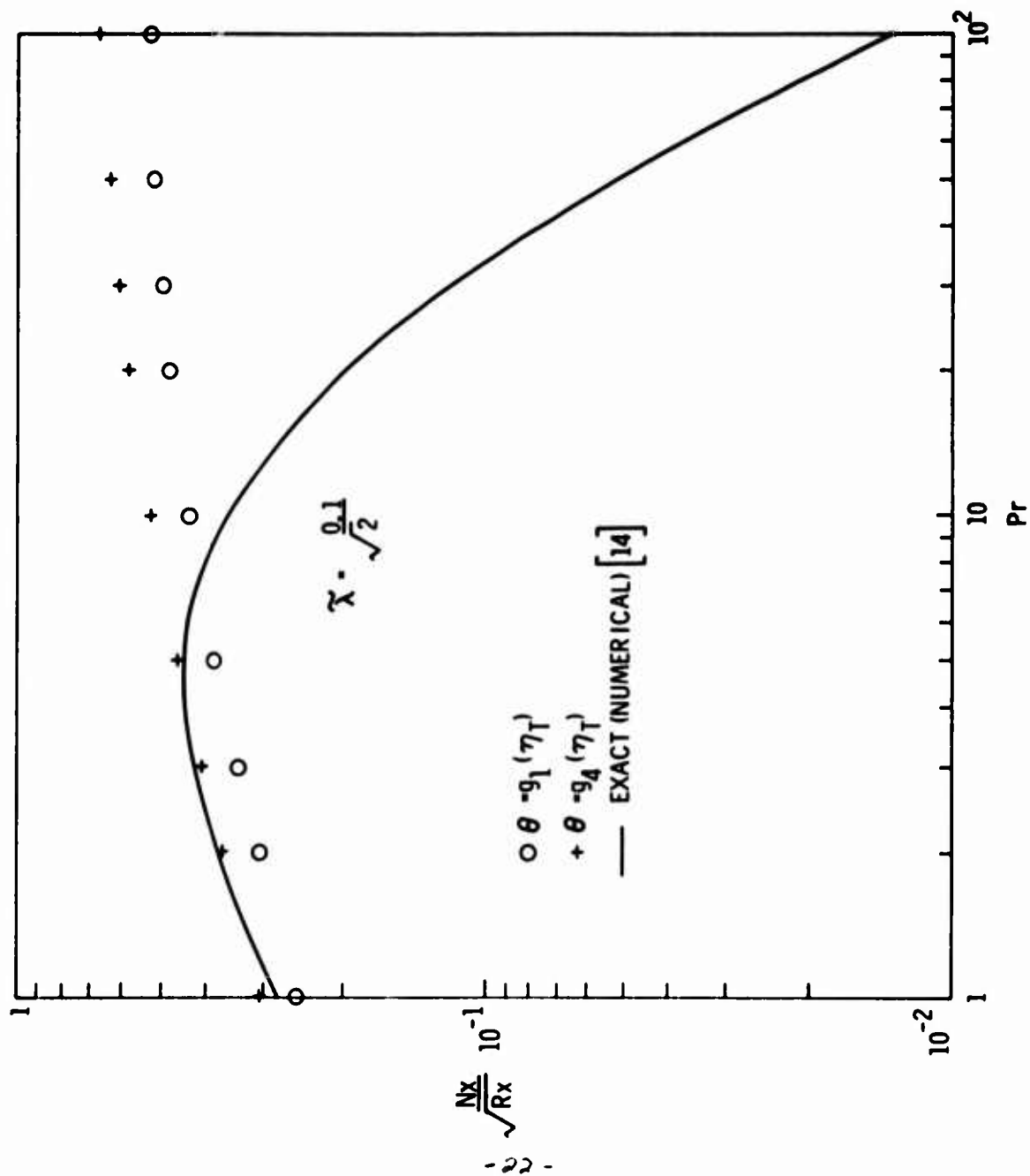


FIG. 5 POROUS PLATE, SIMILARITY BLOWING (USUAL K-P METHOD, $u = y\tau_w/\mu$)

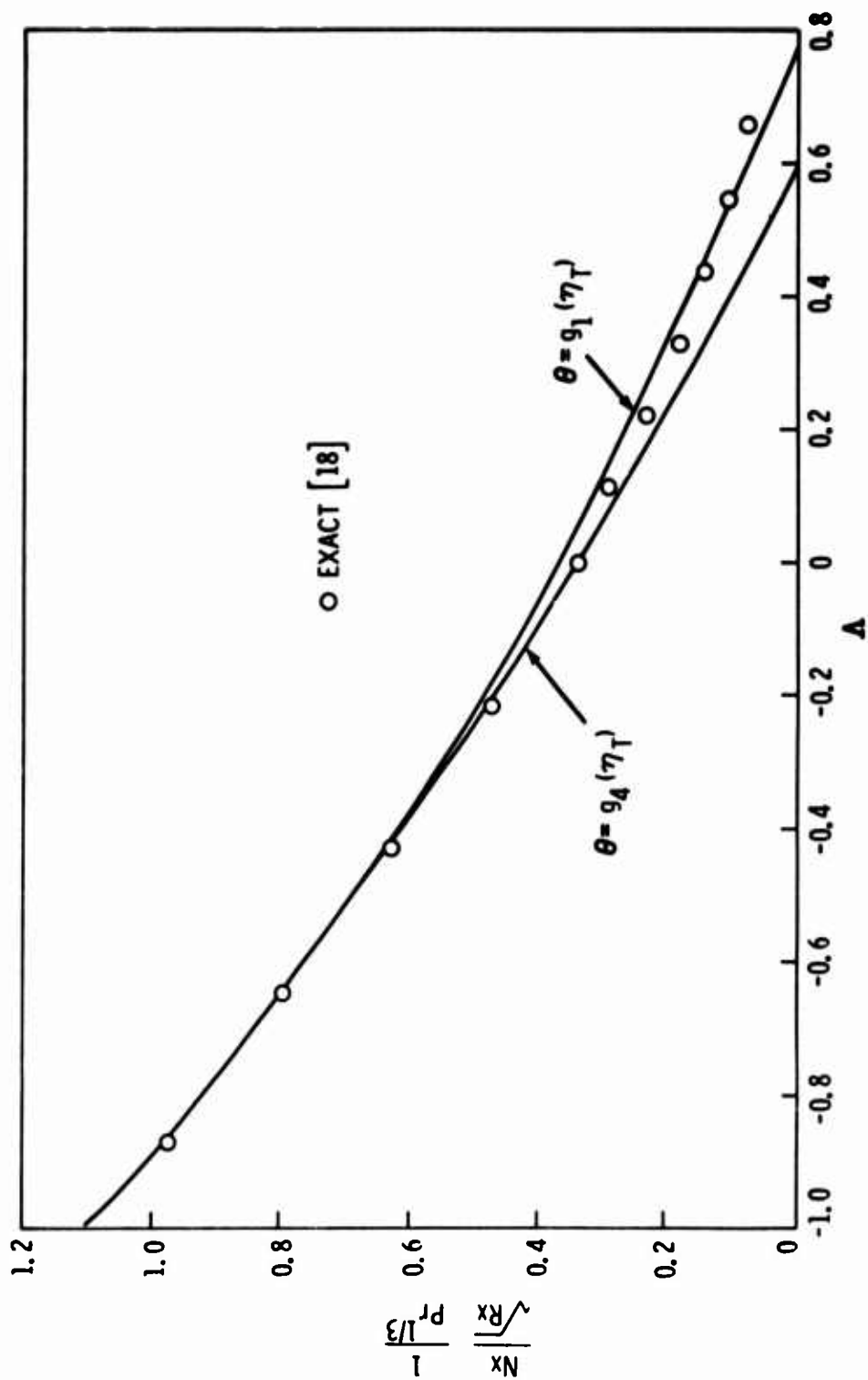


FIG. 6 POROUS PLATE, DISTINGUISHED LIMIT FOR SIMILARITY CASE (PRESENT METHOD)

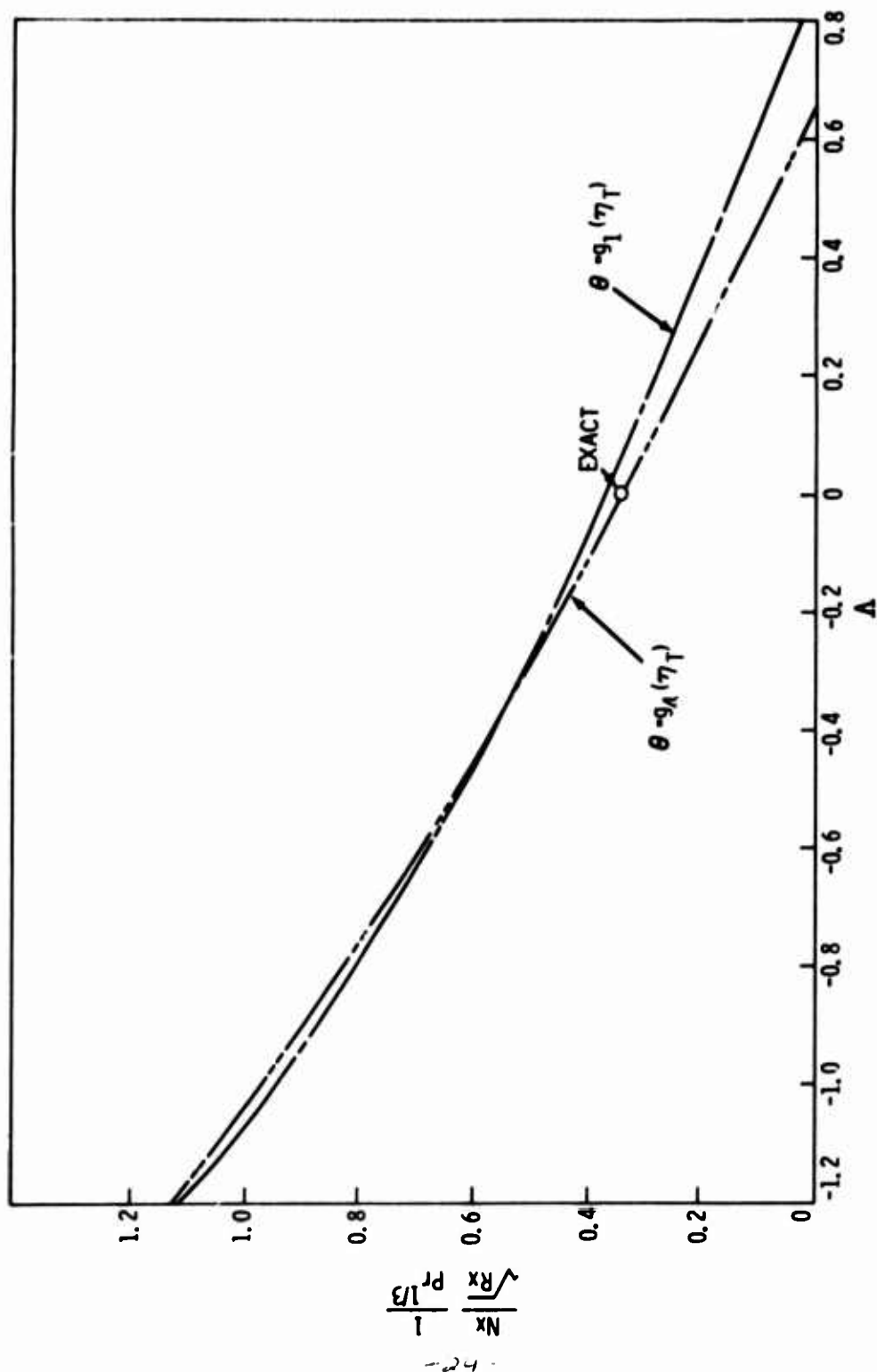


FIG. 7 POROUS PLATE, DISTINGUISHED LIMIT FOR UNIFORM ϵ CASE. (PRESENT METHOD)

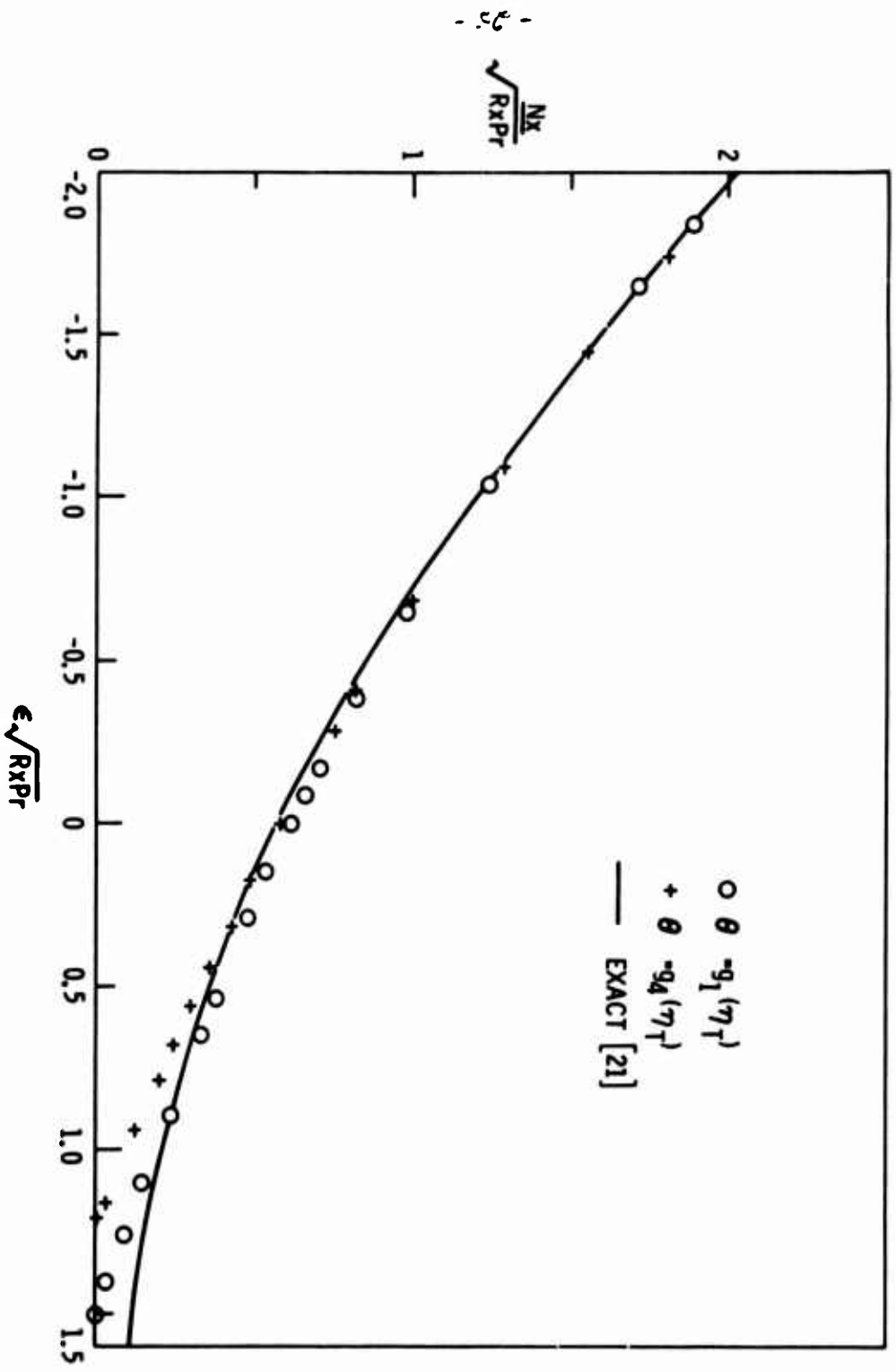


FIG. 8 POROUS PLATE, UNIFORM ϵ , $Pr \rightarrow 0$ (PRESENT METHOD)

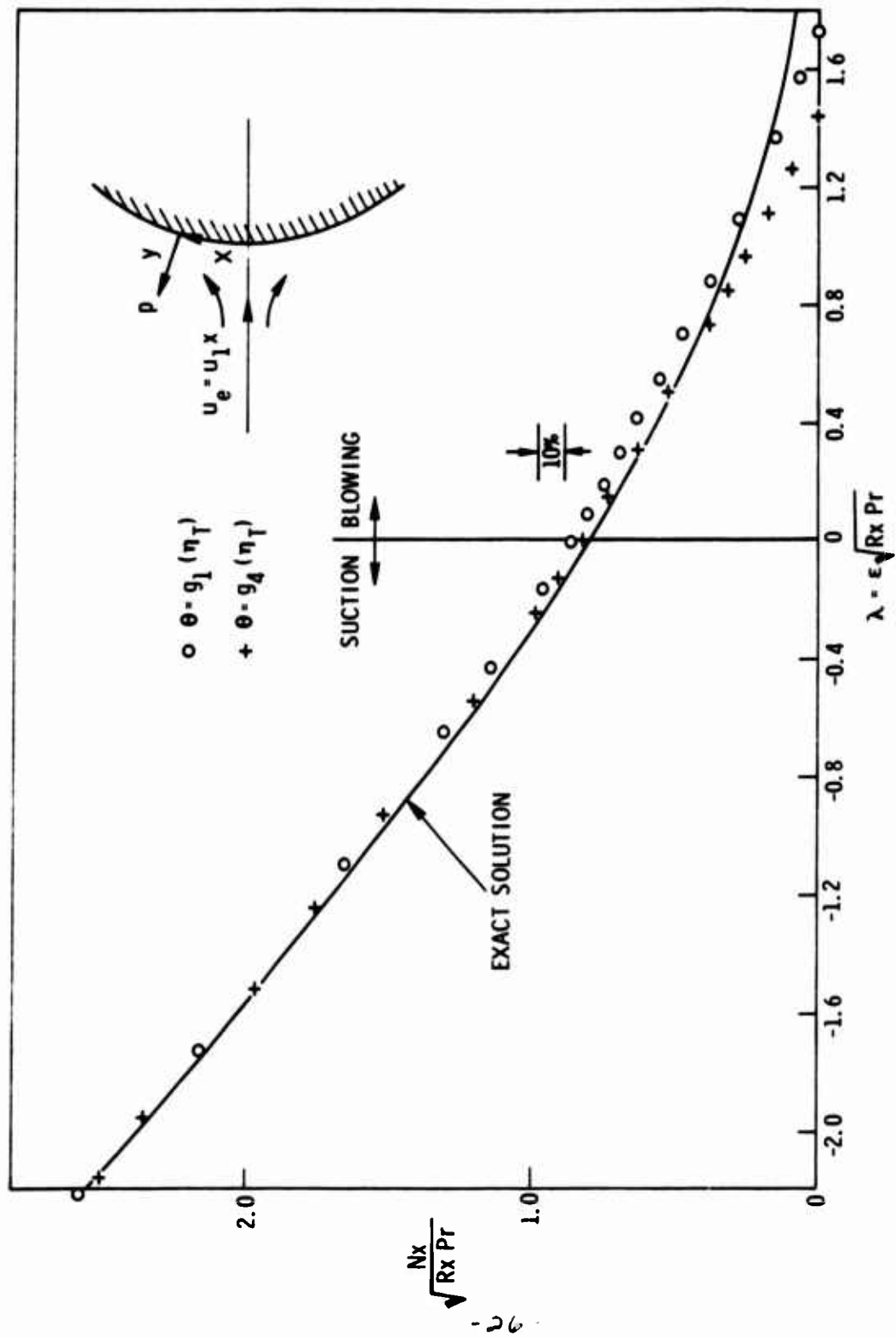


FIG. 9 PLANE STAGNATION POINT, UNIFORM V_w , $Pr \rightarrow 0$ (PRESENT METHOD)